

1 EPN Repro2: A reference GNSS tropospheric dataset over Europe.

2 Rosa Pacione ⁽¹⁾, Andrzej Araszkiewicz ⁽²⁾, Elmar Brockmann ⁽³⁾, Jan Dousa ⁽⁴⁾

3 ⁽¹⁾ e-GEOS S.p.A, ASI/CGS, Italy

4 ⁽²⁾ Military University of Technology, Poland

5 ⁽³⁾ Swiss Federal Office of topography swisstopo

6 ⁽⁴⁾ New Technologies for the Information Society, Geodetic Observatory Pecný, RIGTC, Czech
7 Republic

8 *Correspondence to:* Rosa Pacione (rosa.pacione@e-geos.it)

9 **Abstract.** The present availability of 18+ years of GNSS data belonging to the EUREF Permanent
10 Network (EPN, <http://www.epncb.oma.be/>) is a valuable database for the development of a climate
11 data record of GNSS tropospheric products over Europe. This data record can be used as a reference
12 for a variety of scientific applications and has a high potential for monitoring trend and variability in
13 atmospheric water vapour, improving the knowledge of climatic trends of atmospheric water vapour
14 and being useful for regional Numerical Weather Prediction (NWP) reanalyses as well as climate
15 model simulations. In the framework of the EPN-Repro2, the second reprocessing campaign of the
16 EPN, five Analysis Centres homogenously reprocessed the EPN network for the period 1996-2014.
17 A huge effort has been made for providing solutions that are the basis for deriving new coordinates,
18 velocities and troposphere parameters for the entire EPN. The individual contributions are then
19 combined in order to provide the official EPN reprocessed products. This paper is focused on the
20 EPN Repro2 tropospheric product. The combined product is described along with its evaluation
21 against radiosonde data and European Centre for Medium-Range Weather Forecasts (ECMWF)
22 reanalysis (ERA-Interim) data.

23 1. Introduction

24 The EUREF Permanent Network (Bruyninx et al., 2012; Ihde et al., 2013) is the key geodetic
25 infrastructure over Europe currently made by over 280 continuously operating GNSS reference
26 stations maintained on a voluntary basis by EUREF (International Association of Geodesy Reference
27 Frame Sub-Commission for Europe, <http://www.euref.eu>) members. Since 1996, GNSS data
28 collected at the EUREF Permanent Network have been routinely analysed by several (currently 16)
29 EPN Analysis Centres (Bruyninx C. et al., 2015). For each EPN station, observation data along with
30 metadata information as well as precise coordinates and Zenith Total Delay (ZTD) parameters are
31 publicly available. Since June 2001, the EPN Analysis Centres (AC) routinely estimate tropospheric
32 Zenith Tropospheric Delays (ZTD) in addition to station coordinates. The ZTD, available in daily
33 SINEX TRO files, are used by the coordinator of the EPN tropospheric product to generate each week
34 the final EPN solution containing the combined troposphere estimates with an hourly sampling rate.

35 The coordinates, as a necessary part of this file, are taken from the EPN weekly combined SINEX
36 ([http://www.iers.org/ERS/EN/Organization/AnalysisCoordinator/Sinex Format/sinex.html](http://www.iers.org/ERS/EN/Organization/AnalysisCoordinator/Sinex%20Format/sinex.html)) file.
37 Hence, stations without estimated coordinates in the weekly SINEX file are not included in the
38 combined troposphere solution. The generation of the weekly combined products is done for the
39 routine analysis. Plots of the ZTD time series and ZTD monthly mean as well as comparisons with
40 respect to radiosonde data are available in a dedicated section at the EPN Central Bureau web site
41 (http://www.epncb.oma.be/_productsservices/sitezenithpathdelays/). Radiosonde profiles are
42 provided by EUMETNET as an independent dataset to validate GPS (NAVSTAR Global Positioning
43 System) ZTD data, and are exchanged between EUREF and EUMETNET for scientific purposes
44 based on a Memorandum of Understanding between the two mentioned organisations,
45 (<http://www.euref.eu/documentation/MoU/EUREF-EUMETNET-MoU.pdf>).

46 However, such time series are affected by inconsistencies due to updates of the reference frame and
47 applied models, implementation of different mapping functions, use of different elevation cut-off
48 angles and any other updates in the processing strategies, which causes inhomogeneities over time.
49 To reduce processing-related inconsistencies, a homogenous reprocessing of the whole GNSS data
50 set is mandatory and, for doing it properly, well-documented, long-term metadata set is required.

51 This paper is focused on the tropospheric products obtained in the framework of the second EPN
52 Reprocessing campaign (hereafter EPN-Repro2), where, using the latest available models and
53 analysis strategy, GNSS data of the whole EPN network have been homogeneously reprocessed for
54 the period 1996-2014. The EPN homogeneous long-term GNSS time series can be used as a reference
55 dataset for a variety of scientific applications in meteorological and climate research. Ground-based
56 GNSS meteorology, Bevis et al. (1992), is very well established in Europe and dates back to the 90s.
57 It started with the EC 4th Framework Program (FP) projects WAVEFRONT (GPS Water Vapour
58 Experiment For Regional Operational Network Trials) and MAGIC (Meteorological Applications of
59 GPS Integrated Column Water Vapour Measurements in the western Mediterranean) Project (Haase
60 et al., 2001). Early this century the ability to estimate ZTDs in Near Real Time was demonstrated
61 (COST-716, 2005), and the EC 5th FP scientific project TOUGH (Targeting Optimal Use of GPS
62 Humidity Measurements in Meteorology) funded. Since 2005, the operational production of
63 tropospheric delays has been coordinated and monitored by the EUMETNET EIG GNSS Water
64 Vapour Programme (E-GVAP, 2005-2017, Phase I, II and III, <http://egvap.dmi.dk>). Guerova et al.
65 (2016) report on the state-of-the-art and future prospects of the ground-based GNSS meteorology in
66 Europe. On the other hand, the use of ground-based GNSS long-term data for climate research is still
67 an emerging field.

68 To promote the use of reprocessed long-term GNSS-based tropospheric delay data sets for climate
 69 research is one of the objectives of the Working Group 3 ‘GNSS for climate monitoring’ of the EU
 70 COST Action ES 1206 ‘Advanced Global Navigation Satellite Systems tropospheric products for
 71 monitoring severe weather events and climate (GNSS4SWEC)’, launched for the period of 2013–
 72 2017. The Working Group 3 enforces the cooperation between geodesists and climatologists in order
 73 to generate recommendations on optimal GNSS reprocessing algorithms for climate applications and
 74 standardise the method of conversion between propagation delay and atmospheric water vapour,
 75 Saastamoinen, (1973), Bevis et al., (1992), Bock et al. (2015), with respect to climate standards. For
 76 climate application, maintaining long-term stability is a key issue. Steigenberger et al. (2007) found
 77 that the lack of consistencies over time due to changes in GNSS processing could cause
 78 inconsistencies of several millimetres in GNSS-derived Integrated Water Vapour (IWV) making
 79 climate trend analysis very challenging. Jin et al. (2007) studied the seasonal variability of GPS Zenith
 80 Tropospheric Delay (1994-2006) over 150 international GPS stations and showed the relative trend
 81 in northern hemisphere and southern hemisphere as well as in coastal and inland areas. Wang and
 82 Zhang (2009) derived GPS Precipitable Water Vapour (PWV) using the International GNSS Service
 83 (IGS), Dow et al. (2009), tropospheric products at about 400 global sites for the period 1997-2006
 84 and analysed PWV diurnal variations. Nilsson and Elgered (2008) showed PWV changes from -0.2
 85 mm to +1.0 mm in 10 years by using the data from 33 GPS stations located in Finland and Sweden.
 86 Sohn and Cho (2010) analysed GPS Precipitable Water Vapour trend in South Korea for the period
 87 2000-2009 and examined the relationship between GPS PWV and temperature, which is the one of
 88 the climatic elements. Better information about atmospheric humidity, particularly in climate-
 89 sensitive regions, is essential to improve the diagnosis of global warming, and for the validation of
 90 climate predictions on which socio-economic response strategies are based with strong societal
 91 benefits. Suparta (2012) reported on the validation of PWV as an essential tool for solar-climate
 92 studies over tropical region. Ning et al. (2013) used 14 years of GPS-derived IWV at 99 European
 93 sites to evaluate the regional Rossby Centre Atmospheric (RCA) climate model. GPS monthly mean
 94 data were compared against RCA simulation and the ERA Interim data. Averaged over the domain
 95 and the 14 years covered by the GPS data, they found IWV differences of about 0.47 kg/m² and 0.39
 96 kg/m² for RCA-GPS and ECMWF-GPS, with a standard deviation of 0.98 kg/m² whereas it is 0.35
 97 kg/m² respectively. Using GNSS atmospheric water vapour time series, Alshawaf et al. (2016) found
 98 a positive trend at more than 60 GNSS sites in Europe with an increase of 0.3-0.6 mm/decade with a
 99 temporal increment correlated with the temporal increase in the temperature levels.

100 In this scenario, EPN Repro2 tropospheric product is a unique dataset for the development of a climate
 101 data record of GNSS tropospheric products over Europe, suitable for analysing climate trends and

102 variability, and calibrating/validating independent datasets at global and regional scales. However,
103 although homogenously reprocessed, this time series suffer from site-related inhomogeneity due, for
104 example, to instrumental changes (receivers, cables, antennas, and radomes), changes in the station
105 environment, which can affect the analysis of the long-term variability (Vey et al. 2009). Therefore,
106 to get realistic and reliable climate signals such change points in the time series needs to be detected
107 (Ning et al, 2016a).

108 This paper describes the EPN-Repro2 reprocessing campaign in Section 2. Section 3 is devoted to the
109 combined solutions, i.e. the official EPN-Repro2 products, while in Section 4 the combined solutions
110 is evaluated w.r.t. Radiosonde and ERA-Interim data. Summary and recommendations for future
111 reprocessing campaign are drawn in Section 5.

112 **2. EPN second reprocessing campaign**

113 EPN-Repro2 is the second EPN reprocessing campaign organized in the framework of the special
114 EUREF project “EPN reprocessing”. The first reprocessing campaign, which covered the period
115 1996-2006, Voelksen (2011), involved the participation of all sixteen EPN Analysis Centres (ACs)
116 reprocessing their own EPN sub-network. This guarantees that each site is processed by three ACs at
117 least which is an indispensable condition for proving a combined product. The second reprocessing
118 campaign covered all the EPN stations, which were operated from January 1996 through December
119 2013. Then, participated ACs decided to extend this period until the end of 2014 for troposphere
120 products. Data from about 280 stations in the EPN historical database have been considered. As of
121 December 2014, 23% of EPN stations are between 18-15 years old, 26% are between 14-10 years old,
122 30% between 10-5 years old, and 21% less than 5 years old. Only five, over sixteen, EPN ACs (see
123 Table 1) took part in EPN-Repro2 each providing one reprocessed solution at least. One of the goal
124 of the second reprocessing campaign was to test the diversity of the processing methods in order to
125 ensure verification of the solutions. For this reason, the three main GNSS software packages Bernese
126 (Dach et al., 2014), GAMIT (King et al., 2010) and GIPSY-OASIS II (Webb et al., 1997) have been
127 used to reprocess the whole EPN network and several variants have been provided in addition. In
128 total, eight individual contributing solutions, obtained using different software and settings, and
129 covering different EPN networks, are available. Among them, three are obtained with different
130 software and cover the full EPN network while three are obtained using the same software (namely
131 Bernese) and covering different EPN networks. In Table 2 the processing characteristics of each
132 contributing solution are reported. Despite the software used and the analysed networks, there are a
133 few diversities among the provided solutions, whose impact needs to be evaluated before performing
134 the combination. As far as the GNSS products used in the reprocessing campaign all the ACs used

135 CODE Repro2 product (Lutz et al., 2014) with one exception (see Table 2) where JPL Repro2
136 products (Desai et al., 2014) are used. For tropospheric modelling two mapping functions are used:
137 GMF (Boehm et al., 2006a) and VMF1 (Boehm et al., 2006b), whose impact has been evaluated in
138 Tesmer et al., 2007.

139 **2.1 Impact of GLONASS data**

140 GPS data are used by all ACs in this reprocessing campaign, while two of them (namely IGE and
141 LPT) reprocessed GPS and GLONASS (Global'naja Navigacionnaja Sputnikovaja Sistema)
142 observations. The impact of GLONASS observations has been evaluated in terms of raw differences
143 between ZTD estimates as well as on the estimated linear trend derived from the ZTD time series.
144 Two solutions were prepared and compared. Both were obtained using the same software and the
145 same processing characteristics except the observation data: one with GPS and GLONASS, and one
146 with GPS data only. GLONASS observations are available since 2003, but only from 2008 onwards
147 the amount of GLONASS data (see Figure 1) is significant. The difference in terms of the ZTD trends
148 (Figure 2) between a GPS-only and a GPS+GLONASS solution shows no significant rates for more
149 than 100 stations (rates usually derived from more than 100000 ZTD differences. This indicates that
150 the inclusion of additional GLONASS observations in the GNSS processing has a neutral impact on
151 the ZTD trend analysis. Satellite constellations are continuously changing in time due to satellites
152 being replaced are newly added for all systems. This result is a positive sign that climate trends can
153 be determined independently of the satellite systems used in the processing. In near future the
154 inclusion of additional Galileo (Satellite System in Europe) and BeiDou (Satellite system in China)
155 data will become operational in the GNSS data processing. These data will certainly improve the
156 quality of the tropospheric products but, hopefully, will not introduce systematic changes in terms of
157 ZTD trends as a possible climate indicator.

158 **2.2 Impact of IGS type mean and EPN individual antenna calibration models**

159 According to the processing options listed in the EPN guidelines for the Analysis Centre
160 (http://www.epncb.oma.be/_documentation/guidelines/guidelines_analysis_centres.pdf), when
161 available EPN individual antenna calibration models have to be used instead of IGS type mean
162 calibration models. Currently, individual antenna calibration models are available at about 70 EPN
163 stations. As reported in Table 2 there are individual solutions carried out with IGS type mean antenna
164 calibration models (Schmid et al., 2015) only and others with IGS type mean plus EPN individual
165 antenna calibration models. It may happen that for the same station there are contributing solutions
166 obtained applying different antenna models. To evaluate the impact of using these different antenna
167 calibration models on the ZTD, two solutions were prepared and compared. Both were obtained using

the same software and the same processing characteristics except the calibration models. First one used the IGS type mean models only, while second one used the individual calibrations whenever it was possible and IGS type mean for the rest of the antennas. An example of the time series of the ZTD difference obtained applying ‘Individual’ and ‘Type Mean’ antenna calibration models for the EPN station KLOP (Kloppenheim, Frankfurt, Germany) is shown in Figure 3. KLOP station is included in the EPN network since June, 2nd 2002, a TRM29659.00 antenna with no radome was installed. Two instrumentation changes occurred at the station: the first in June 27th 2007, when the previous antenna was replaced with a TRM55971.00 and a TZGD radome, the second in June 28th 2013 with the installation of a TRM57971.00 and a TZGD radome. For all of them the individual calibrations are available through the data sets compiled by the EPN Central Bureau (ftp://epncb.oma.be/pub/station/general/epnc_08.atx). Switching between phase centre corrections from type mean to individual (or vice versa) causes a disagreement in the estimated height of the stations, as it mentioned by Araszkiewicz and Voelksen (2016), as well as in their ZTD time series. Depending on the antenna model, the offset at station KLOP in the up component is -5.2 ± 0.5 mm, 8.7 ± 0.6 mm and 5.6 ± 0.8 mm with a corresponding offset in the ZTD of 0.2 ± 0.5 mm, -1.5 ± 0.5 mm, -1.4 ± 0.8 mm, respectively. Similar situation appears also for all stations/antennas for which individual calibration models are available. The corresponding offset in the ZTD has opposite sign for the antennas with offset in the up component larger than 5 mm (16 antennas) and, generally, not exceeding 2 mm for ZTD. Such inconsistency in the ZTD time series are not large enough to be captured during the combination process (see Section 3) where 10 mm threshold in the ZTD bias (about 1.5 kg/m^2 IWV) is set in order to flag problematic ACs or stations.

2.3 Impact of non-tidal atmospheric loading

As reported in the IERS Convention (2010), the diurnal heating of the atmosphere causes surface pressure oscillations at diurnal S1, semidiurnal S2, and higher harmonics. These atmospheric tides induce periodic motions of the Earth's surface (Petrov and Boy, 2004). The conventional recommendation is to calculate the station displacement using the Ray and Ponte (2003) S2 and S1 tidal model. However, crustal motion related to non-tidal atmospheric loading has been detected in station position time series from space geodetic techniques (van Dam et al., 1994; Magiarotti et al., 2001, Tregoning and Van Dam, 2005). Several models of station displacements related to this effect are currently available. Non-tidal atmospheric loading models are not yet considered as Class-1 models by the International Earth Rotation and Reference Systems Service (IERS 2010) indicating that there are currently no standard recommendations for data reduction. To evaluate their impact, two solutions, one without and one with non-tidal atmospheric loading, have been compared for the

201 year 2013. In the last one, the National Centers for Environmental Prediction (NCEP) model is used
202 at the observation level during data reduction (Tregoning and Watson, 2009).

203 Dach et al. (2010) have already found that the repeatability of the station coordinates improves by
204 20% when applying the effect directly on the data analysis and by 10% when applying a post-
205 processing correction to the resulting weekly coordinates compared with a solution without
206 considering these corrections. However, the effect of applying non-tidal atmospheric loading on the
207 ZTD seems to be negligible. Generally, it causes a difference below 0.5 mm with a scattering not
208 larger than 0.3 mm. The difference is thus below the level of confidence. Figure 4 shows time series
209 of the differences of the ZTD and up component between two time series obtained with and without
210 non-tidal atmospheric loading for two EPN stations: KIR0 (Kiruna, Sweden) and RIGA (Riga, Latvia).
211 There is also no correlation between values of estimated differences and vertical displacements
212 caused by non-tidal atmospheric loading. Correlation coefficients for analysed EPN stations were
213 below 0.2.

214 **3. EPN Repro2 combined solutions**

215 The EPN ZTD combined product is obtained applying a generalized least square approach following
216 the scheme described in Pacione et al. (2011). The first step in the combination process is reading and
217 checking the SINEX TRO files delivered by the ACs. At this stage, gross errors (i.e. ZTD estimates
218 with formal sigma larger than 15 mm) are detected and removed. The combination starts if at least
219 three different solutions are available for a single site. Then, a first combination is performed to
220 compute proper weights for each contributing solution to be used in the final combination step. In
221 this last step the combined ZTD estimates, their standard deviations and site/AC specific biases are
222 determined. The combination fails if, after the first or second combination level, the number of ACs
223 become less than three. Finally, ZTD site/AC specific biases exceeding 10 mm are investigated as
224 potential outliers.

225 The EPN-Repro2 combination activities were carried out in two steps. First, a preliminary combined
226 solution for the period 1996-2014 was performed taken as input all the available eight homogeneously
227 reprocessed solutions (see Table 2). The aim of this preliminary combined solution is to assess each
228 contributing solution and to investigate site/AC specific biases prior to the final combination, flag the
229 outliers and send a feedback to the ACs. The agreement of each contributing solution w.r.t. the
230 preliminary combination is given in terms of bias and standard deviation (not showed) As far as the
231 standard deviation is concerned, it is generally below 2.5 mm with a clear seasonal behaviour, while
232 the bias is generally in the range of +/- 2 mm. However, there are several GPS weeks for which the
233 bias and standard deviation values exceeded the before mentioned limits. To investigate these outliers,

the time series of site/AC specific bias has been studied, since it can be a useful tool to detect bad periods of data and provide information useful for cleaning the EPN historical archive. An example is given in Figure 5 for the station VENE (Venice, Italy) for three contributing solutions AS0, GO4 and MU2 (G00 and GO1 are not shown but are very close to GO4). In the first years of acquisition, tracking issues were experienced at VENE, which are clearly mirrored in the bias time series.

All the site/AC specific biases are divided into three groups: the red group contains site/AC specific biases whose values are larger than 25 mm, the orange group contains site/AC specific biases in the range of [15 mm, 25 mm] and the yellow group contains site/AC specific biases in the range of [10 mm, 15 mm]. In Table 3 summarizes percentages of red, orange and yellow biases for each contributing solution. The majority of biases belong to the yellow group; the percentage of biases in the orange group ranges from 12% for LP0 and LP1 solutions to 27% for AS0 solution, while percentage of biases in the red group ranges from 3% for MU4 solution to 22% for IG0 solution.

The final EPN Repro2 tropospheric combination is based on the following input solutions: AS0, GO4, IG0, LP1 and MU2. MUT AC provided the MU2 solution after the preliminary combination, its only difference with respect to MU4 is the use of type mean antenna and individual calibration models, whose effect is shown in section 2.2. The agreement in terms of bias and standard deviation of each contributing solution w.r.t. the final combination is shown in Figure 6. As regard as the standard deviation, there is a clear improvement with respect to the preliminary combination due to the removal of the outliers detected during the preliminary combination. The standard deviation is below 3 mm from GPS week 835-1055 and 2 mm after. This is somehow related to the worse quality of data and products during the first years of the EPN/IGS activities.

The final EPN Repro2 tropospheric combination is consistent to the final coordinate combination performed by the EPN Analysis Centre Coordinator. During the coordinate combination all stations were analyzed by comparing their coordinates for specific ACs and the preliminary combined values. In case where the differences were larger than 16 mm in the up component, the station was eliminated and the whole combination was repeated, up to three times, if necessary. This ensures the consistency of final coordinates at the level of 16 mm in the up component (Figure 7). As a rule of thumb, 9 mm in the height component (i.e. 3 mm in ZTD as explained in Santerre, 1991) are needed to fulfill the requirement of retrieving IWV at an accuracy level of 0.5 kg/m² (Bevis et al., 1994), Ning et al (2016b). As shown in Figure 7, only one site, MOPI (Modra Piesok, Slovakia), exceed this threshold on a long term. As reported at the EPN Central Bureau, MOPI has been excluded several times from the routine combined solutions. MOPI has very bad periods of observations in past due to radome

manipulation that caused jumps in the height component. However, several stations exceeded it temporary during bad periods, as shown in Figure 8 for VENE (Venezia, Italy).

4. Evaluation of the ZTD Combined Products with respect to independent data set

The evaluation with respect to other sources or products, such as Radiosonde data from the E-GVAP and numerical weather re-analysis from the European Centre for Medium-Range Weather Forecasts, ECMWF (ERA-Interim), provides a measure of the accuracy of the ZTD combined products.

4.1 Evaluation versus radiosonde

For the GPS and Radiosonde comparisons at the EPN collocated sites, we used profiles from the World Meteorological Organization provided by EUMETNET in the framework of the Memorandum of Understanding between EUREF and EUMETNET. Radiosonde profiles are processed using the software (Haase et al., 2003) that checks the quality of the profiles, converts the dew point temperatures to specific humidity, transforms the radiosonde profile to correct for the altitude offset between the GPS and the radiosonde sites and determines ZTD, ZWD and IWV compensating for the change of gravitational acceleration, g , with height.

Figure 9 shows an example for the EPN site CAGL (Cagliari, Sardinia Island, Italy). For all the 183 EPN collocated sites, and using all the data available in the considered period, we computed an overall bias and standard deviation (Figure 10). The sites are sorted according to the increasing distances from the nearest Radiosonde launch site. MALL (Palma de Mallorca, Spain) is the closest (0.5 km to Radiosonde code 8301) while GRAZ (Graz, Austria) is the most distant (133 km to Radiosonde code 14015). The amount of data available for the comparisons varies between sites depending on the availability of the GPS and Radiosonde ZTD estimates in the considered epoch and it ranges from 121 for VIS6 (Visby, Sweden, integrated in the EPN since 22-06-2014) up to 21226 for GOPE (Ondrejov, Czech Republic, integrated in the EPN since 31-12-1995).

The bias ranges from -0,87%, which corresponds to -21,2 mm, (at EVPA, Ukraine, and distance from the Radiosonde launch site 96.5 km, Radiosonde code 33946) to 0,68%, which corresponds to 15,4 mm, (at OBER, Germany, and distance from the Radiosonde launch site 90.8 km, Radiosonde code 11120). The mean bias for all sites is -0,6 mm with standard deviation of 4.9 mm. For the more than 75% (178 pairs), the agreement is below 5 mm and only 5.5% (13 pairs) have bias higher than 10 mm. The higher biases concern mostly the pairs over 50 km away from each other, like GPS stations OBER, OBE2 and OBET located in Oberpfaffenhofen (Germany) and collocated with Radiosonde (VRS90L code 11120) launched from Innsbruck Airport in Austria on the opposite side of North Chain in the Karwendel Alps. Our results are at odds with Wang et al. (2007), where authors compared PW from GPS and global Radiosonde. In contrast to them, we received small negative bias

299 -1.19 mm for Vaisala Radiosondes, which is the most common type used in Europe (81% of all used
 300 in this study). For MRZ, GRAW and M2K2 Radiosonde type, which represent 4.6%, 3.4% and 3.0%
 301 of compared Radiosondes respectively, we received systematic positive bias. However, Wang et al.
 302 (2007) used global Radiosonde data from 2003 and 2004, while we used all available data over
 303 Europe from 1994 to 2015. This can partly explain the disagreement even though more analysis
 304 deserves to be done. Further investigation is also needed for several near or moved GPS stations. For
 305 example in Brussels (Belgium) BRUS station, included in the EPN network since 1996, was replaced
 306 by BRUX in 2012. Their bias w.r.t. the same Radiosonde (VRS80L code 6447) has opposite sign (-
 307 1.2 mm and 3.4 mm respectively). A possible explanation is the different time span over which the
 308 bias has been computed (1996-2012 for BRUS, 2012-2015 for BRUX).

309 In agreement with Ning et al. 2012, the standard deviation generally increases with the distance from
 310 the Radiosonde launch site. It is in the range of [0,16; 0,76] % ,which corresponds to [3; 18] mm, till
 311 15 km (first band in Figure 10); [0,29;0,78] % ,which corresponds to [7; 19] mm, till 70 km (second
 312 band in Figure 10) and [10; 33] mm till 133 km (third band in Figure 10). The evaluation of the
 313 standard deviation is comparable with previous studies. Haase et al. (2001) showed very good
 314 agreement with biases less than 5 mm and the standard deviation of 12 mm for most of analysed sites
 315 in Mediterranean. Similar results ($6.0 \text{ mm} \pm 11.7 \text{ m}$) were obtained also by Vedel et al. (2001). Both
 316 of them based on non-located pairs distant less than 50 km. Pacione et al (2011), considering 1-
 317 year of GPS ZTD and Radiosonde data over the E-GVAP super sites network, obtained a standard
 318 deviation of 5-14 mm. Dousa et al. 2012 evaluated ZTD and Radiosonde on a global scale over 10-
 319 month period and reported a standard deviation of 5–16 mm.

320 The assessment of the EPN Repro1 ZTD product with respect to Radiosonde using the same period,
 321 i.e. 1996-2014 when completed with the EUREF operational product after GPS week 1407
 322 (December 30, 2006), and EPN Repro2 with respect to the Radiosonde data has an improvement of
 323 approximately 3-4% in the overall standard deviation.

324 **4.2 Evaluation versus ERA-Interim data**

325 ERA-Interim (Dee et al., 2011) from the European Centre for Medium-Range Weather Forecasts
 326 (ECMWF) are used as Numerical Weather Prediction (NWP) model data. The ERA-Interim is a re-
 327 analysis product available every 6 hours (00, 06, 12, 18 UTC) with a horizontal resolution of 1×1
 328 degree and 60 vertical model levels.

329 For the period 1996-2014 and for each EPN station, ZTD and tropospheric linear horizontal gradients
 330 were computed using the GFZ (German Research Centre for Geosciences) ray-tracing software (Zus
 331 et al., 2014). Combined EUREF Repro1 and Repro2 products as well as individual ACs tropospheric

parameters were assessed with the corresponding parameters estimated from the NWM re-analysis. The evaluation of GNSS and NWM was performed using the GOP-TropDB (Gyori and Dousa, 2016) via calculating parameter differences for pairs of stations using values at every 6 hours (00:00, 6:00, 12:00 and 18:00) as available from the NWM product. A linear interpolation from values ± 30 min was thus necessarily applied for all GNSS products providing HH:30 timestamps as required for the combination process. As all compared GNSS products has the same time resolution (1 hour), the interpolation is assumed to affect all products in the same way. Therefore, we assume all inter-comparisons to a common reference (NWM) principally reflects the quality of the products. No vertical corrections were applied since NWM parameters were estimated for the long-term antenna reference position of each station.

Table 4 summarizes the mean total statistics of individual (ACs) and combined (EUREF) tropospheric parameters, ZTDs and horizontal gradients, over all available stations. The EUREF combined solution does not provide tropospheric gradients and these could be evaluated for individual solutions only. In Table 4, we can observe a common ZTD bias of about -1.8 mm for all GNSS solutions compared to the ERA-Interim, however still highly varying for individual stations as obvious from estimated uncertainties. ZTD standard deviations are generally at the level of 8 mm between GNSS and NWM products, but for IG0 solution performing about 25% worse than others as already detected during the combination. Two solutions, AS0 and LP1 are slightly better than GO4 and MU2 – reaching the standard deviation of 7.7 mm their accuracy is at the level of the EUREF combined solution. The better performance of the AS0 solution can be considered due to its theoretical better capability of the modelling true dynamics in the troposphere as the solution applied a stochastic troposphere modelling using undifference observations sensitive to the absolute tropospheric delays. On the other hand, LP1 included roughly one third from of EPN stations which were properly selected according to the station quality thus making a difficulty to interpret the difference with respect to those processing full EPN.

The comparison of tropospheric linear horizontal gradients (East and North) from GNSS and NWM revealed a problem with the MU2 solution showing a high inconsistency of results over different stations, which is not visible in the total statistics, but mainly in the uncertainties by an order higher compared to all others. Geographical plot (not showed) confirmed this site-specific systematic, but in both positive and negative senses. The impact was however not observed in MU2 ZTD results. Additionally, the GO4 solution performed slightly worse than the others. It was identified as a consequence of estimating 6-hour gradients using the piece-wise linear function and without any absolute or relative constraints. In such case, higher correlations with other parameters occurred

365 raising uncertainties of the estimates. For this purpose, the GO6 solution (not showed) was derived
 366 fully compliant with the GO4, but stacking tropospheric gradients into 24 hours piece-wise linear
 367 modelling. By comparing the GO6 (Dousa and Vaclavovic, 2016), the standard deviations dropped
 368 from 0.38 mm to 0.28 mm and from 0.40 mm to 0.29 mm for East and North gradients, respectively
 369 which corresponds to the LP1 solution applying the same settings. Additionally, Dousa and
 370 Vaclavovic, 2016 found a strong impact of a low-elevation receiver tracking problem on estimation
 371 of horizontal gradients which was particularly visible when compared to the ERA-Interim. Systematic
 372 behaviour in monthly mean difference in gradient seems to be a useful indicator for instrumentation-
 373 related issues and should be applied as one of the tools for cleaning the EPN historical archive.

374 For completeness, we evaluated also EPN Repro1 ZTD product with respect to the ERA-Interim
 375 using the same period, i.e. 1996-2014 when completed with the EUREF operational product after
 376 GPS week 1407 (December 30, 2006). Comparing EPN Repro1 and EPN Repro2 with the numerical
 377 weather re-analysis showed the 8-9% improvement of the latter in both overall standard deviation
 378 and systematic error. Figure 11 shows distributions of station means and standard deviations of EPN
 379 Repro1 and EPN Repro2 ZTDs compared to NWM ZTDs using the whole period 1996-2014.
 380 Common reductions of both statistical characteristics are clearly visible for the majority of all stations.
 381 From data of Figure 11, we also expressed site-by-site improvements in terms of ZTD bias, standard
 382 deviation and RMS (Figure 12). Calculated medians reached 21.1 %, 6.8 % and 8.0 %, respectively,
 383 which corresponds to the abovementioned improvement of 8-9 %. The degradation of standard
 384 deviation was found at three stations: SKE8 (Skellefteaa, Sweden, integrated in the EPN since 28-09-
 385 2014), GARI (Porto Garibaldi, Italy, integrated in the EPN since 08-11-2009) and SNEC (Snezka,
 386 Czech Republic, former EPN station since 14-06-2009) all of them providing much less data
 387 compared to others, 1%, 30% and 3%, respectively. All other stations (290) showed improvements.
 388 We also found 72 stations with increased absolute bias in EUREF Repro1 compared to Repro2 while
 389 all others, 221 stations (75%), resulted in reduced systematic error.

390 Time series of monthly mean biases and standard deviations for ZTD differences of EPN Repro2 and
 391 the ERA-Interim is showed in Figure 13. The small negative bias slowly decreases towards 2014, but
 392 a high uncertainty of the mean indicates site-specific behaviour depending mainly on latitude and
 393 altitude of the EPN station and the quality of both NWM and GNSS products. There is almost no
 394 seasonal signal observed in time series of ZTD mean biases or the uncertainty, but clearly in ZTD
 395 standard deviation and the uncertainty. Slightly increasing standard deviation towards 2014 can be
 396 attributed to the increase of number of stations in EPN starting from about 30 in 1996 and with more

397 than 250 in 2014. More stations reduces a variability in monthly mean biases, however, site-specific
398 errors then contribute more to higher values of standard deviation.

399 Figure 14 displays the geographical distribution of total ZTD biases and standard deviations for all
400 sites. Prevailing negative biases seem to become lower or even positive in the mountain areas. There
401 is no latitudinal dependence observed for ZTD biases in Europe, but a strong one for standard
402 deviations. This corresponds mainly to the increase of water vapour content and its variability towards
403 the equator.

404 **5. Conclusion**

405 In this paper, we described the activities carried out in the framework of the EPN second reprocessing
406 campaign. We focused on the tropospheric products homogeneously reprocessed by five EPN Analysis
407 Centres for the period 1996-2014 and we described the ZTD combined products.

408 Both individual and combined tropospheric products along with reference coordinates and other
409 metadata, are stored in SINEX TRO format, Gendt, G. (1997), and are available to the users at the
410 EPN Regional Data Centres (RDC), located at BKG (Federal Agency for Cartography and Geodesy,
411 Germany). For each EPN station, plots on ZTD time series, ZTD monthly mean, comparison versus
412 Radiosonde data (if collocated), and comparison versus the ERA-Interim data will be available at the
413 EPN Central Bureau (Royal Observatory of Belgium, Brussels, Belgium).

414 Assessment of the EPN Repro1 and Repro2 with respect to the Radiosonde data has an improvement
415 of approximately 3-4% in the overall standard deviation.

416 Assessment of the EPN Repro1 and Repro2 with respect to the ERA-Interim re-analysis showed the
417 8-9% improvement of the latter over the former in both overall standard deviation and systematic
418 error which was obvious for majority of the stations. Comparisons of the GNSS solutions with the
419 NWM, i.e. independent source, showed the overall agreement at the level of 8-9 mm, however, rather
420 site-specific ranging from 5 mm to 15 mm for standard deviations and from -7 mm to 3 mm for biases
421 considering 99% of results roughly.

422 The use of ground-based GNSS long-term data for climate research is an emerging field. For the
423 assessment of Euro-CORDEX (Coordinated Regional Climate Downscaling Experiment) climate
424 model simulation IGS Repro1, Byun and Bar-Sever, (2009), has been used as reference reprocessed
425 GPS products (Bastin et al. 2016). However, this data set is quite sparse over Europe (only 85 stations
426 over the 280 EPN stations) and covers the period 1996-2010. According to Wang et al. (2007) IGS
427 ZTD products are valuable source of water vapor data for climate and weather studies. The GPS PW
428 is useful also for monitoring the quality of the radiosonde data. However, a better spatial coverage of

the GNSS PW data is needed to investigate and reduce systematic biases in comparison with the global radiosonde humidity data (Wang and Zhang, 2009). On the other hand extending the observation period and complement of temporal coverage is necessary to calculate more reliable mean values and trends. As it was pointed by Baldysz et al. (2015, 2016) additional two years of ZTD data can change estimated trends up to 10%. Therefore, data after 2010 and with a better coverage over Europe are required for improving the knowledge of climatic trends of atmospheric water vapour in Europe. In this scenario, EPN-Repro2 can be used as a reference data set with a high potential for monitoring trend and variability in atmospheric water vapour.

Considering five EPN stations, among those with the longest time span, GOPE (Ondrejov, Czech Republic, integrated in the EPN since 31-12-1995), METS (Kirkkonummi, Finland, integrated in the EPN since 31-12-1995), ONSA (Onsala, Sweden, integrated in the EPN since 31-12-1995), PENC (Penc, Hungary, integrated in the EPN since 03-03-2006) and WTZR (Bad Koetzting, Germany, integrated in the EPN since 31-12-1995), we have computed ZTD trends using EPN Repro2, EPN Repro1 completed with the EUREF operational products, radiosonde and ERA-Interim data. All of them are also in the IGS Network, for which IGS Repro1 completed with the IGS operational products are available and extracted from the GOP-TropDB. First we have removed annual signal from the original time series and marked all outliers according to 3-sigma criteria. Then for all GPS ZTD data sets we have estimated all well-known and recognized shifts related to the antenna replacement. No other unexplained breaks has been removed to be sure that we not introduce any artificial errors. Based on the cleaned and filtered data we have used linear regression model before and after the considered epoch independently. The difference between those two models in specific epoch is considered as a shift. Then, we have removed all the estimated shifts from the original time series. Generally, the size of the shifts is much lower than noise level and depends on the applied method of its estimation. Therefore, the final results are affected by used methodology and cannot be considered as an absolute values. No homogenization has been done for radiosonde since radiosonde metadata are not available. Finally, a LSE method have been applied to estimate linear trends and seasonal component. ZTD trends (Figure 15) for all three GPS ZTD data sets are consistent, as soon as the same homogenisation procedure is applied. Then overall RMS is 0.02 mm/year. Among all five ZTD sourced, we find the best agreement for ONSA (RMS=0.04mm/year) and WTZR (RMS=0.02mm/year). For PENC we have good agreement with respect to ERA-Interim (0.05 mm/year), but a large discrepancy versus radiosonde (-0.31 mm/year). This large discrepancy is probably due to the distance to the radiosonde launch site (40.7 km, radiosonde code 12843) and to the lack of the homogenisation stage. Over the five considered stations the agreement with respect to ERA-Interim (RMS = 0.11 mm/year) is better than that with respect to radiosonde (RMS = 0.16

463 mm/year). Even though for the five considered stations EPN Repro2 do not change significantly the
464 detection of ZTD trends, it has a better agreement with respect to radiosonde and ERA-Interim data
465 than EPN Repro1. It has also the best spatial resolution than IGS Repro1 and radiosonde data, which
466 are used today for long-term analysis over Europe. Taking into account the good consistency among
467 trends, EPN Repro2 can be used for trend detection in areas where other data are not available.

468 Comparisons with regional climate model simulations is one of the application of EPN-Repro2.
469 Ongoing at Sofia University is comparison between GNSS IWV, computed from EPN-Repro2 ZTD
470 data for SOFI (Sofia, Bulgaria), and ALADIN-Climate IWV simulations conducted by the Hungarian
471 Meteorological Service, for the period 2003-2008. The preliminary results show a tendency of the
472 model to underestimate IWV. Clearly, larger number of model grid points need to be investigated in
473 different regions in Europe and the EPN-Repro2 data is well suited for this. Climate research is not
474 only limited to comparison with climate model and derivation of trends. At the Met Office, the UK's
475 national weather service, within the framework of the European FP7 project UERRA (Uncertainties
476 in Ensembles of Regional Re-analysis, <http://www.uerra.eu/>), assimilation trials of reprocessed ZTD
477 into a 12 km European climate reanalysis beginning in 1979 are ongoing. To account for any
478 systematic bias or bias change, the reprocessed ZTDs will have a bias correction applied before
479 assimilation.

480 The reprocessing activity of the five EPN ACs was a huge effort generating homogeneous products
481 not only for station coordinates and velocities, but also for tropospheric products. The knowledge
482 gained will certainly help for a next reprocessing activity. A next reprocessing will most likely
483 include Galileo and BeiDou data and therefore it will be started in some years from now after having
484 successfully integrated these new data in the current operational near real-time and daily products of
485 EUREF. The consistent use of identical models in various software packages is another challenge for
486 the future to be able to improve the consistency of the combined solution. Prior any next reprocessing,
487 it was agreed in EUREF to focus on cleaning and documenting data in the EPN historical archive as
488 it should highly facilitate any future work. For this purpose, all existing information need to be
489 collected from all the levels of data processing, combination and evaluation which includes initial
490 GNSS data quality checking, generation of individual daily solutions, combination of individual
491 coordinates and ZTDs, long-term combination for velocity estimates and assessments of ZTDs and
492 gradients with independent data sources.

493

494 *Author Contributions.* R. Pacione coordinated the writing of the manuscript and wrote section 1, 2, 3
495 and 4.1. A. Araszkiewicz wrote section 2.2 and 2.3. E. Brockmann wrote section 2.1. J. Dousa wrote section

496 4.2. All authors contributed to section 5. All authors approved the final manuscript before its
497 submission.

498

499 **Acknowledgments**

500 The authors would like to acknowledge the support provided by COST - -European Cooperation in
501 Science and Technology for providing financial assistance for publication of the paper. The
502 authors thank the members of the EUREF project “EPN reprocessing”. e-GEOS work is done
503 under ASI Contract 2015-050-R.0. The assessments of the EUREF combined and individual
504 solutions in the GOP-TropDB were supported by the Ministry of Education, Youth and Science,
505 the Czech Republic (project LH14089). The MUT AC contribution was supported by statutory
506 funds at the Institute of Geodesy, Faculty of Civil Engineering and Geodesy, Military University
507 of Technology (No. PBS/23-933/2016). Finally, we thank the two anonymous referees and the
508 Associate Editor Dr. Roeland Van Malderen for their comments which helped much to improve
509 the paper.

510

511 **References**

- 512 Alshawaf, F., Dick, G., Heise, S., Simeonov, T., Vey, S., Schmidt, T., and Wickert, J.: Decadal
513 variations in atmospheric water vapor time series estimated using ground-based GNSS, *Atmos. Meas.*
514 *Tech. Discuss.*, doi: 10.5194/amt-2016-151, in review, 2016.
- 515 Araszkiewicz, A., and Voelksen, C.: The impact of the antenna phase center models on the
516 coordinates in the EUREF Permanent Network, *GPS Solution*, doi: 10.1007/s10291-016-0564-7,
517 2016.
- 518 Baldysz, Z., Nykiel, G., Figurski, M., Szafranek, K., and Kroszczynski, K.: Investigation of the 16-
519 year and 18-year ZTD Time Series Derived from GPS Data Processing. *Acta Geophys.* 63, 1103-
520 1125, DOI: 10.1515/acgeo-2015-0033, 2015.
- 521 Baldysz Z., Nykiel G., Araszkiewicz A., Figurski M. and Szafranek K.: Comparison of GPS
522 tropospheric delays derived from two consecutive EPN reprocessing campaigns from the point of
523 view of climate monitoring. *Atmos. Meas. Tech.*, 9, 4861-4877, DOI: 10.5194/amt-9-4861-2016,
524 2016.
- 525 Bastin, S., Bock, O., Chiriaco, M., Conte, D., Dominguez, M., Roehring, R., Drobinski, P., Parracho,
526 A.: Evaluation of MED-CORDEX simulations water cycle at different time scale using long-term
527 GPS-retrieved IWV over Europe, presentation at COST ES1206 workshop, Potsdam (Germany) 1-2
528 September 2016.
- 529 Bevis, M., Businger, S., Herring, T. A., Rocken C., Anthes, R. A., and Ware, R. H.: GPS Meteorology:
530 Remote Sensing of 20 Atmospheric Water Vapour Using the Global Positioning System, *J. Geophys.*
531 *Res.*, 97, 15787–15801, 1992.

532 Bevis M., S. Businger, S. Chiswell, T. A. Herring, R. A. Anthes, C. Rocken, and Ware, R. H.: GPS
533 Meteorology: Mapping Zenith Wet Delays onto Precipitable Water. *Journal of Applied Meteorology*,
534 33, 379-386, 1994.

535 Byun S. H., and Bar-Sever, Y. E.: A new type of troposphere zenith path delay product of the
536 International GNSS Service. *J Geodesy*, 83(3-4), 1–7, 2009.

537 Bock, O., P. Bosser, R. Pacione, M., Nuret, N. Fourrie, and Parracho, A.: A high quality reprocessed
538 ground-based GPS dataset for atmospheric process studies, radiosonde and model evaluation, and
539 reanalysis of HYMEX Special Observing Period, *Quarterly Journal of the Royal Meteorological*
540 *Society*, doi: 10.1002/qj.2701, 2015.

541 Boehm, J., and Schuh, H.: Vienna mapping functions in VLBI analyses, *Geophys. Res. Lett.*, 31,
542 L01603, doi: 10.1029/2003GL018984, 2004.

543 Boehm, J., A. Niell, P. Tregoning, and Schuh, H.: Global Mapping Function (GMF): A new empirical
544 mapping function based on numerical weather model data, *Geophys. Res. Lett.*, 33, L07304, doi:
545 10.1029/2005GL025546, 2006a.

546 Boehm, J., B. Werl, and Schuh, H.: Troposphere mapping functions for GPS and very long baseline
547 interferometry from European Centre for Medium-Range Weather Forecasts operational analysis data,
548 *J. Geophys. Res.*, 111, B02406, doi: 10.1029/2005JB003629, 2006b.

549 Bruyninx C, Habrich H, Söhne W, Kenyeres A, Stangl G, Völkse C (2012) Enhancement of the
550 EUREF Permanent Network Services and Products, *Geodesy for Planet Earth*, IAG Symposia Series,
551 136: 27–35. doi: 10.1007/978-3-642-20338

552 Bruyninx, C., A. Araszkiewicz, E. Brockmann, A. Kenyeres, R. Pacione, W. Söhne, G. Stangl, K.
553 Szafranek, and Völkse, C.: EPN Regional Network Associate Analysis Center Technical Report
554 2015, IGS Technical Report 2015, Editors Yoomin Jean and Rolf Dach, Astronomical Institute,
555 University of Bern, 2015, pp. 101-110, 2015.

556 COST-716 Exploitation of Ground-Based GPS for Operational Numerical Weather Prediction and
557 Climate Applications – Final Report, in: Elgered, G., Plag, H.-P., Van der Marel, H., et al. (Eds.),
558 EUR 21639, 2005.

559 Dach, R., Hugentobler, U., Fridez, P., and Meindl, M.: Bernese GPS Software Version 5.0, *Journal*
560 *of Geophysical Research Atmospheres*, 119, doi: 10.1002/2013JD021124, 2014.

561 Dach, R., J. Böhm, S. Lutz, P. Steigenberger and Beutler, G.: Evaluation of the impact of atmospheric
562 pressure loading modeling on GNSS data analysis, *J Geod* doi: 10.1007/s00190-010-0417-z, 2010.

563 Dee, D. P., S. M. Uppala, A. J. Simmons, P. Berrisford, P. Poli, S. Kobayashi, U. Andrae, M. A.
564 Balmaseda, G. Balsamo, P. Bauer, P. Bechtold, and Beljaars, A. C. M.: The ERA-Interim reanalysis:
565 Configuration and performance of the data assimilation system, *Q. J. Roy. Meteor. Soc.*, 137(656),
566 553–597, 2011.

567 Desai, S. D., W. Bertiger, M. Garcia-Fernandez, B. Haines, N. Harvey, C. Selle, A. Sibthorpe, A.
568 Sibois, and Weiss, J. P.: JPL's Reanalysis of Historical GPS Data from the Second IGS Reanalysis
569 Campaign, AGU Fall Meeting, San Francisco, CA, 2014.

570 Dow, J.M., Neilan, R. E., and Rizos, C.: The International GNSS Service in a changing landscape of
571 Global Navigation Satellite Systems, *Journal of Geodesy* 83:191–198, doi: 10.1007/s00190-008-
572 0300-3, 2009.

573 Dousa, J. and G.V. Bennett: Estimation and Evaluation of Hourly Updated Global GPS Zenith Total
574 Delays over ten Months, *GPS Solutions*, Online publication date: 12-Oct-2012, doi:10.1007/s10291-
575 012-0291-7, 2012.

576 Dousa, J. and Vaclavovic P.: The GOP troposphere product from the 2nd European re-processing
577 (1996-2014), 2016 (manuscript prepared for AMT)

578 Gendt, G. SINEX TRO—Solution (Software/technique) INdependent Exchange Format for
579 combination of TROpospheric estimates Version 0.01, March 1,
580 1997:https://igscb.jpl.nasa.gov/igscb/data/format/sinex_tropo.txt, 1997.

581 Gyori G, and Douša J.: GOP-TropDB developments for tropospheric product evaluation and
582 monitoring – design, functionality and initial results, In: IAG Symposia Series, Rizos Ch. and Willis
583 P. (eds), Springer Vol. 143, pp. 595-602., 2016

584 Guerova, G., J. Jones, J. Douša, G. Dick, S. de Haan, E. Pottiaux, O. Bock, R. Pacione, G. Elgered,
585 H. Vedel, and M. Bender: Review of the state-of-the-art and future prospective of GNSS Meteorology
586 in Europe, accepted for publication in to Special Issue: Advanced Global Navigation Satellite
587 Systems tropospheric products for monitoring severe weather events and climate (GNSS4SWEC),
588 (AMT/ACP/ANGEo inter-journal SI), 2016.

589 IERS Conventions (2010). Gérard Petit and Brian Luzum (eds.). (IERS Technical Note ; 36) Frankfurt
590 am Main: Verlag des Bundesamts für Kartographie und Geodäsie, 2010. 179 pp., ISBN 3-89888-989-
591 6, 2010.

592 Ihde, J., Habrich, H., Sacher, M., Söhne, W., Altamimi, Z., Brockmann, E., Bruyninx, C., Caporali,
593 C., Dousa, J., Fernandes, R., Hornik, H., Kenyeres, A., Lidberg, M., Mäkinen, J., Poutanen, M.,
594 Stangl, G., Torres, J.A., Völksen, C., (2013). EUREF's contribution to national, European and global
595 geodetic infrastructures. *IAG Symposia*, vol. 139, pp. 189–196. doi: 10.1007/978-3-642-37222-3_24.

596 Jin, S.G., J. Park, J. Cho, and P. Park: Seasonal variability of GPS-derived Zenith Tropospheric Delay
597 (1994-2006) and climate implications, *J. Geophys. Res.*, 112, D09110, doi: 10.1029/2006JD007772,
598 2007.

599 Haase, J., Calais, E., Talaya, J., Rius, A., Vespe, F., Santangelo, R., Huang, X.-Y., Davila, J. M., Ge,
600 M., Cucurull, L., Flores, A., Sciarretta, C., Pacione, R., Bocolari, M., Pugnaghi, S., Vedel, H.,
601 Mogensen, K., Yang, X., and Garate, J.: The contributions of the MAGIC project to the COST 716
602 objectives of assessing the operational potential of ground-based GPS meteorology on an
603 international scale, *Physics and Chemistry of the Earth, Part A*, 26, 433–437, 2001.

604 Haase, J.S., H. Vedel, M. Ge, and E. Calais: GPS zenith tropospheric delay (ZTD) variability in the
605 Mediterranean, *Phys Chem Earth (A)* 26(6–8):439–443, 2001.

606 Haase, J., M. Ge, H. Vedel, and Calais, E.: Accuracy and variability of GPS Tropospheric Delay
607 Measurements of Water Vapor in the Western Mediterranean, *Journal of Applied Meteorology*, 42,
608 1547-1568, 2003.

609 King, R., Herring, T., and McClusky, S.: Documentation for the GAMIT GPS analysis software 10.4.,
610 Tech. rep., Massachusetts Institute of Technology, 2010.

611 Lutz, S., P. Steigenberger, G. Beutler, S. Schaer, R. Dach, and Jaggi, A.: GNSS orbits and ERPs from
612 CODE's repro2 solutions, IGS Workshop Pasadena (USA), June 23–27, 2014.

613 Nilsson, T. and Elgered, G.: Long-term trends in the atmospheric water vapor content estimated from
614 ground-based GPS data. *J. Geophys. Res.*, 113, doi: 10.1029/2008JD010110, 2008.

615 Ning, T., R. Haas, G. Elgered, and. Willén U: Multi-technique comparisons of 10 years of wet delay
616 estimates on the west coast of Sweden, *J Geod* 86: 565. doi: 10.1007/s00190-011-0527-2, 2012.

617 Ning, T., J. Wickert, Z. Deng, S. Heise, G. Dick, S. Vey, and Schone, T.: Homogenized time series
618 of the atmospheric water vapor content obtained from the GNSS reprocessed data, *Journal of Climate*,
619 doi: 10.1175/JCLI-D-15-0158.1, 2016a

620 Ning, T., J. Wang, G. Elgered, G. Dick, J. Wickert, M. Bradke, M. Sommer, R. Querel, and Smale,
621 D.: The uncertainty of the atmospheric integrated water vapour estimated from GNSS observations
622 *Atmos. Meas. Tech.*, 9, 79-92, doi:10.5194/amt-9-79-2016, 2016b.

623 Mangiarotti, S., A. Cazenave, L. Soudarin and Crétaux, J. F.: Annual vertical crustal motions
624 predicted from surface mass redistribution and observed by space geodesy, *Journal of Geophysical*
625 *Research*, 106, B3, 4277, 2001.

626 Pacione, R., B. Pace, S.de Haan, H. Vedel, R.Lanotte, and Vespe, F.: Combination Methods of
627 Tropospheric Time Series, *Adv. Space Res.*, 47(2) 323-335 doi: 10.1016/j.asr.2010.07.021, 2011.

628 Petrov, L. and Boy, J.-P.: Study of the atmospheric pressure loading signal in very long baseline
629 interferometry observations," *J. Geophys. Res.*, 109, B03405, 14 pp., doi: 10.1029/2003JB002500,
630 2004.

631 Ray, R. D. and Ponte, R. M.: Barometric tides from ECMWF operational analyses, *Ann. Geophys.*,
632 21(8), pp. 1897-1910, doi: 10.5194/angeo-21-1897-2003.

633 Saastamoinen, J.: Contributions to the theory of atmospheric refraction, *Bull. Geodes.*, 107, 13–34,
634 doi:10.1007/BF02521844, 1973.

635 Santerre R.: Impact of GPS Satellite sky distribution. *Manuscr. Geod.*, 16, 28-53, 1991.

636 Schmid R, Dach R, Collilieux X, Jäggi A, Schmitz M, Dilssner F (2015) Absolute IGS antenna phase
637 center model igs08.atx: status and potential improvements. *J Geod* 90(4):343–364

638 Sohn, D.-H., and Cho, J.: Trend Analysis of GPS Precipitable Water Vapor Above South Korea Over
639 the Last 10 Years, *J. Astron. Space Sci.* 27(3), 231-238 (2010), doi: 10.5140/JASS.2010.27.3.231,
640 2010.

641 Suparta, W.: Validation of GPS PWV over UKM Bangi Malaysia for climate studies, *Procedia*
642 *Engineering* 50, 325 – 332, 2012.

643 Steigenberger, P., V. Tesmer, M. Krugel, D. Thaller, R. Schmid, S. Vey, and Rothacher, M.:
644 Comparisons of homogeneously reprocessed GPS and VLBI long time-series of troposphere zenith
645 delays and gradients, *J. Geod.*, 81(6-8), 503–514, doi: 10.1007/s00190-006-0124-y, 2007.

646 Tesmer, V., J. Boehm, R. Heinkelmann and Schuh, H.: Effect of different tropospheric mapping
647 functions on the TRF, CRF and position time-series estimated from VLBI, *Journal of Geodesy* June
648 2007, Volume 81, Issue 6, pp 409-421, 2007.

649 Tregoning, P. and Van Dam, T.: Atmospheric pressure loading corrections applied to GPS data at the
650 observation level, *Geophysical Research Letters*, 32, 22, 2005.

651 Tregoning P., Watson C.: Atmospheric effects and spurious signals in GPS analyses. *J. Geophys.*
652 *Res.*, 114, B09403, doi: 10.1029/2009JB006344, 2009.

653 Van Dam, T., G. Blewitt, and Heflin, M. B.: Atmospheric pressure loading effects on Global
654 Positioning System coordinate determinations, *Journal of Geophysical Research*, 99, B12, 23939,
655 1994.

656 Vey, S., R. Dietrich, M. Fritsche, A. Rulke, P. Steigenberger, and Rothacher, M.: On the homogeneity
657 and interpretation of precipitable water time series derived from global GPS observations, *J. Geophys.*
658 *Res.*, 114, D10101, doi: 10.1029/2008JD010415, 2009.

659 Voelksen, C.: An update on the EPN Reprocessing Project: Current Achievements and Status,
660 Presented at EUREF 2011 Symposium, Chisinau, Republic of Moldova, May 25-28 2011,
661 [http://www.epncb.oma.be/_documentation/papers/eurefsymposium2011/an_update_on_epn_reproc](http://www.epncb.oma.be/_documentation/papers/eurefsymposium2011/an_update_on_epn_reprocessing_project_current_achievement_and_status)
662 [essing_project_current_achievement_and_status](http://www.epncb.oma.be/_documentation/papers/eurefsymposium2011/an_update_on_epn_reprocessing_project_current_achievement_and_status), 2011.

663 Wang, J., Zhang, L., Dai. A., Van Hove, T., Van Baelen, J.: A near-global, 2-hourly data set of
664 atmospheric precipitable water dataset from ground-based GPS measurements, *J Geophys Res*
665 112(D11107). doi:10.1029/2006JD007529, 2007.

666 Wang, J. and Zhang, L.: Climate applications of a global, 2-hourly atmospheric precipitable water
667 dataset derived from IGS tropospheric products, *J Geod* 83: 209. doi: 10.1007/s00190-008-0238-5,
668 2009.

669 Webb, F. H., and Zumberge, J.F.: An Introduction to GIPSY/OASIS II. JPL D-11088, 1997.

670 Vedel, H., K. S. Mogensen, and X.-Y. Huang: Calculation of zenith delays from meteorological data
671 comparison of NWP model, radiosonde and GPS delays, *Phys. Chem. Earth Pt. A*, 26, 497–502, doi:
672 10.1016/S1464-1895(01)00091-6, 2001.

673 Zus, F, Dick, G, Heise, S, Dousa, J, and Wickert J.: The rapid and precise computation of GPS slant
674 total delays and mapping factors utilizing a numerical weather model, *Radio Sci*, 49(3): 207-216, doi:
675 10.1002/2013RS005280, 2014.

676

677 **Table**

678 **Table Captions**

679 Table 1: EPN Analysis Centres providing EPN Repro2 solutions.

680 Table 2: EPN Repro2 processing options for each contributing solutions. AS0 solutions provided by
681 ASI/CGS (Matera, Italy), GO0, GO1 and GO4 solutions provided by GOP (Pecny, Czech Republic),
682 IG0 solution provided by IGE (Madrid, Spain), LP0 and LP1 solutions provided by LPT (Waben,
683 Switzerland), MU2 and MU4 solutions provided by MUT (Warsaw, Poland).

684 Table 3. Percentage of red, orange and yellow bias for each contributing solution.

685 Table 4. Mean statistics and uncertainties, calculated from results of individual stations, provided
686 for AC individuals and EUREF combined (Repro1 and Repro2) tropospheric parameters compared
687 to the ERA-Interim re-analysis.

AC	Full name	City	Country	SW	EPN Network
ASI	Agenzia Spaziale Italiana	Matera	Italy	GIPSY-OASIS II	Full EPN
GOP	Geodetic Observatory	Pecny	Czech Republic	Bernese	Full EPN
IGE	National Geographic Institute	Madrid	Spain	Bernese	EPN-Subnetwork
LPT	Federal Office of Topography	Wabern	Switzerland	Bernese	EPN-Subnetwork
MUT	Military University of Technology	Warsaw	Poland	GAMIT	Full EPN

Table 1: EPN Analysis Centres providing EPN Repro2 solutions.

	AS0	GO0	GO1	GO4	IG0	LP0	LP1	MU2	MU4
SW	GIPSY 6.2	Bernese 5.2			Bernese 5.2	Bernese 5.2		GAMIT 10.5	
GNSS	G	G			G + R	G + R		G	
SOLUTION TYPE	PPP	Network			Network	Network		Network	
STATIONS	Full EPN	Full EPN			EPN Subnetwork	EPN Subnetwork		Full EPN	
ORBITS	JPL R2	CODE R2			CODE R2	CODE R2		CODE R2	
ANTENNAS	IGS08	IGS08 + Individual.			IGS08+ Individual.	IGS08	IGS08 + Individual.	IGS08 + Individual.	IGS08
IERS	2010	2010			2010	2010		2010	
GRAVITY	EGM08	EGM08			EGM08	EGM08		EGM08	
TROPOSPHERE Estimated Parameters	ZTD (5min) GRAD (5min)	ZTD (1h) GRAD (6h)			ZTD (1h) GRAD (6h)	ZTD (1h) GRAD (24h)		ZTD (1h) GRAD (24h)	
MAPPING FUNCTION	VMF1	GMF	VMF1	VMF1	GMF	GMF	VMF1	VMF1	
ZTD/GRAD time stamp	hh:30 24 estimates/day	hh:30 (and hh:00) 24(+24) estimates/day			hh:30 24 estimates/day	hh:30 (and hh:00) 24(+24) estimates/day		hh:30 24 estimates/day	
IONOSPHERE	HOI included	CODE, HOI included			CODE (HOI included)	CODE (HOI included)		CODE IONEX + IGRF11 (HOI included)	
REFERENCE. FRAME	IGb08	IGb08			IGb08	IGb08		IGb08	
OCEAN TIDES	FES2004	FES2004			FES2004	FES2004		FES2004	
TIDAL-ATMOSPHERIC LOADING	NO	NO			YES	YES	YES	YES	
NON-TIDAL-ATMOSPHERIC LOADING	NO	NO	NO	YES	NO	NO	YES	NO	
ELEVATION CUTOFF	3	3			3	3		5	
Delivered SNX_TRO Files [from week to week]	0834-1824	0836-1824			0835-1816	0835-1802		0835-1824	

Table 2: EPN Repro2 processing options for each contributing solutions. AS0 solutions provided by ASI/CGS (Matera, Italy), GO0, GO1 and GO4 solutions provided by GOP (Pecny, Czech Republic), IG0 solution provided by IGE (Madrid, Spain), LP0 and LP1 solutions provided by LPT (Waben, Switzerland), MU2 and MU4 solutions provided by MUT (Warsaw, Poland).

Solution	%Red bias	% Orange bias	% Yellow bias
AS0	17	27	56
G00	10	22	67
G01	12	23	65
G04	12	23	65
IG0	22	14	64
LP0	10	12	79
LP1	10	12	78
MU2	3	15	82

696 Table 3. Percentage of red, orange and yellow bias for each contributing solution.

697

Solution	ZTD bias [mm]	ZTD sdev [mm]	EGRD bias [mm]	EGRD sdev [mm]	NGRD bias [mm]	NGRD sdev [mm]
AS0 (full EPN)	-1.7±2.0	7.7±1.9	0.00±0.06	0.32±0.09	0.09±0.06	0.33±0.10
GO4 (full EPN)	-1.9±2.4	8.1±2.1	-0.04±0.09	0.38±0.10	0.00±0.09	0.40±0.12
MU2 (full EPN)	-1.8±2.0	8.3±2.1	-0.03±0.32	0.35±2.46	-0.01±0.84	0.34±2.37
IG0 (part EPN)	-1.6±2.3	10.7±2.2	-0.05±0.09	0.33±0.11	0.04±0.12	0.36±0.12
LP1 (part EPN)	-1.7±2.4	7.7±1.7	-0.02±0.06	0.28±0.05	0.03±0.09	0.27±0.06
EUR Repro2	-1.8±2.1	7.8±2.2	-	-	-	-
EUR Repro1	-2.2±2.3	8.5±2.1	-	-	-	-

Table 4. Mean statistics and uncertainties, calculated from results of individual stations, provided for AC individuals and EUREF combined (Repro1 and Repro2) tropospheric parameters compared to the ERA-Interim re-analysis.

702 **Figure**

703 **Figure Captions**

704 Figure 1. Time series of the number of GNSS observations for the period 1996-2014. GPS
705 observations are shown in red, GPS+GLONASS in blue and their differences in green. The difference
706 is significant starting 2008.

707 Figure 2. ZTD trend difference GPS – GPS/GLO, computed over 111 sites. The rate in violet (primary
708 y-axis) and the number of used difference is in green (secondary y-axis).

709 Figure 3. EPN station KLOP (Kloppenheim, Frankfurt, Germany) ZTD time series difference
710 between ‘individual’ and ‘type mean’ calibration model. Two instrumentation changes occurred at
711 the station (marked by red lines): the first in June 27th 2007, when the previous antenna was replaced
712 with a TRM55971.00 and a TZGD radome, the second in June 28th 2013 with the installation of a
713 TRM57971.00 and a TZGD radome.

714 Figure 4. Left part: Time series of the ZTD and up component differences between two time series
715 obtained with and without Non-Tidal Atmospheric Loading for two EPN stations: KIRO (Kiruna,
716 Sweden) and RIGA (Riga, Latvia).

717 Figure 5 VENE (Venice Italy) time series of bias and standard deviation for the three contributing
718 solutions AS0, GO4 and MU4 for the period July 21st, 1996 - July 28, 2007 (GPS week 0863-1437).
719 GO0 and GO1 are not shown since they are very close to GO4.

720 Figure 6 Weekly mean bias (upper part) and standard deviation (lower part) of each contribution
721 solutions w.r.t. the final EPN Repro2 combination.

722 Figure 7. The final consistency in up component for all stations. Stations are sorted by name.

723 Figure 8 VENE (Venice Italy) time series of total consistency in up component for the period July
724 21st, 1996 - July 28, 2007 (GPS week 0863-1437).

725 Figure 9 EPN station CAGL (Cagliari, Sardinia Island, Italy). Upper part: Radiosondes (in red) and
726 GPS (in blue) ZTD time series. Lower part differences.

727 Figure 10 GPS versus Radiosonde Bias. The error bar is the standard deviation. Sites are sorted
728 according to the increasing distances from the nearest Radiosonde launch site.

729 Figure 11: Distributions of station means (left) and standard deviations (right) of EPN Repro1 and
730 Repro2 ZTDs compared to ERA-Interim ZTDs.

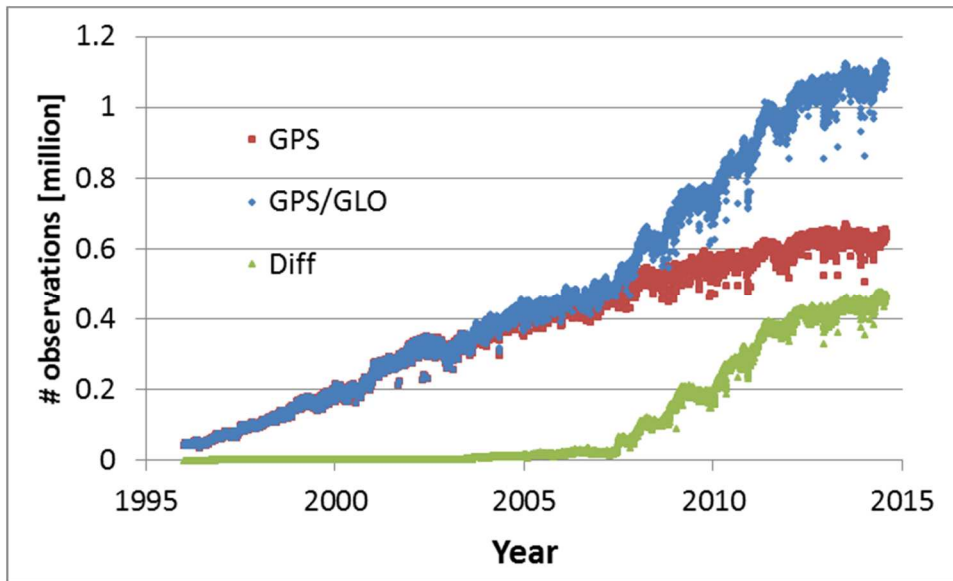
731 Figure 12: Site-by-site ZTD improvements of EPN Repro2 versus EPN Repro1 compared to ERA-
732 Interim

733 Figure 13: Time series of monthly mean biases (lower part) and standard deviations (upper part) for
734 ZTD differences of EPN Repro2 and NWM re-analysis. Uncertainties are calculated over all stations.

735 Figure 14: Geographical display of ZTD biases (left) and standard deviations (right) for EPN Repro2
736 products compared to the ERA-Interim.

737 Figure 15: ZTD trend comparisons at five EPN stations. The error bars are the formal error of the
738 trend values.

739



740

741

742

743

744

Figure 1. Time series of the number of GNSS observations for the period 1996-2014. GPS observations are shown in red, GPS+GLONASS in blue and their differences in green. The difference is significant starting 2008.

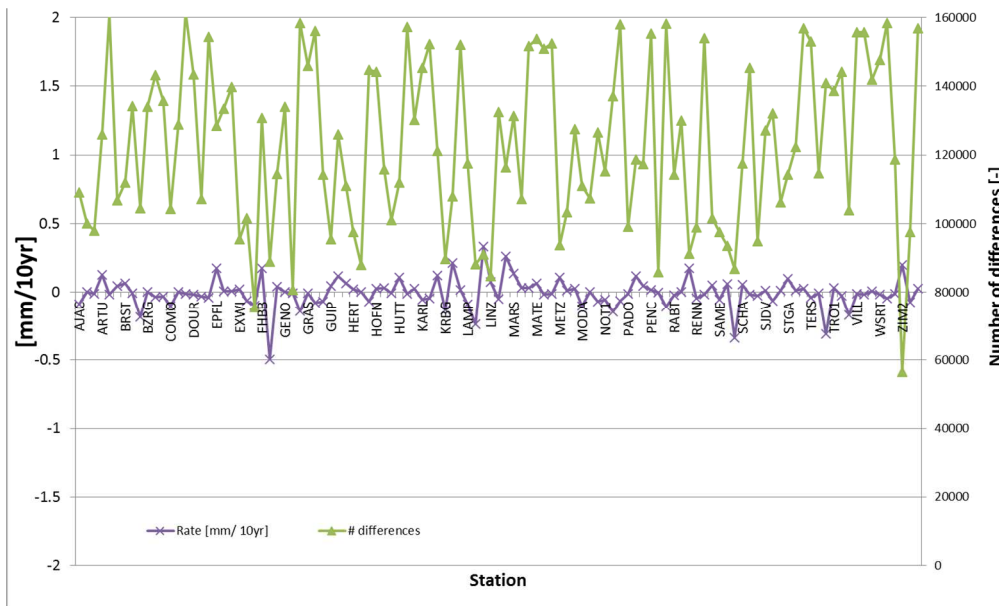
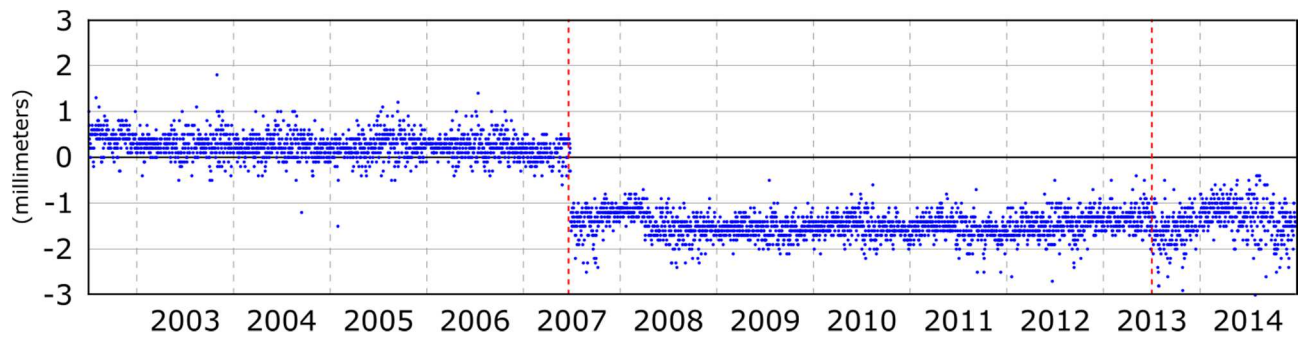


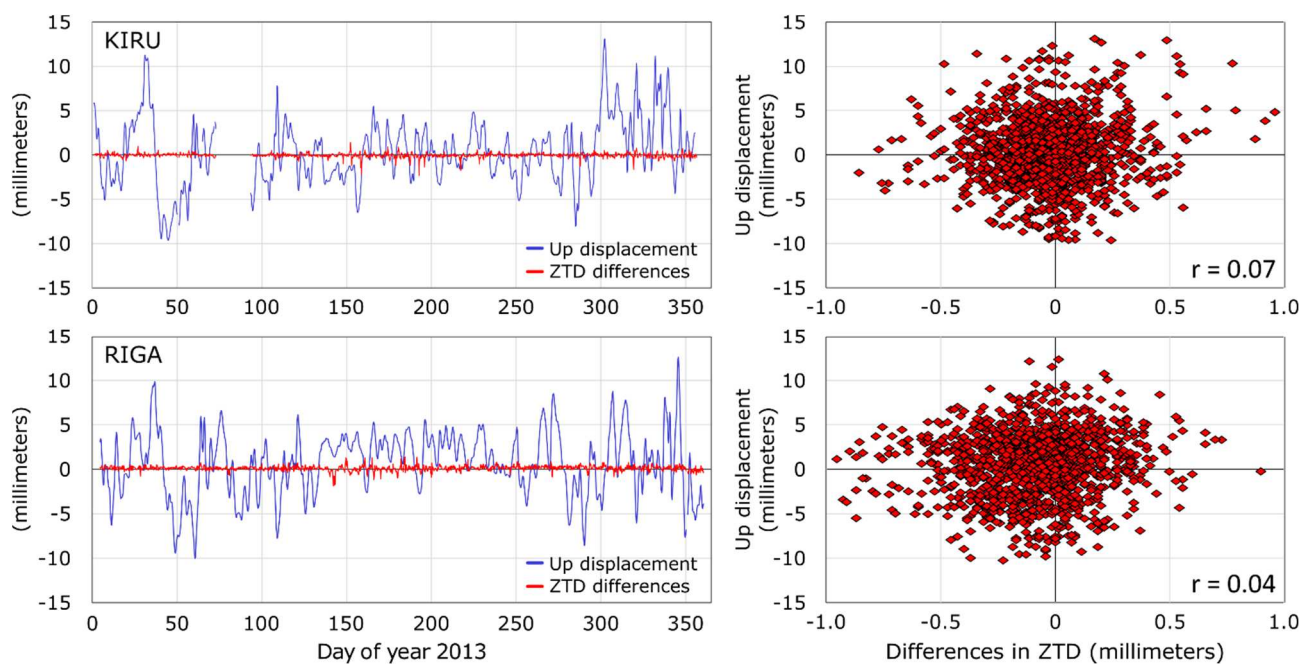
Figure 2. ZTD trend difference GPS – GPS/GLO, computed over 111 sites. The rate in violet (primary y-axis) and the number of used difference is in green (secondary y-axis).



749

750 Figure 3. EPN station KLOP (Kloppenheim, Frankfurt, Germany) ZTD time series difference
 751 between ‘individual’ and ‘type mean’ calibration model. Two instrumentation changes occurred at
 752 the station (marked by red lines): the first in June 27th 2007, when the previous antenna was replaced
 753 with a TRM55971.00 and a TZGD radome, the second in June 28th 2013 with the installation of a
 754 TRM57971.00 and a TZGD radome.

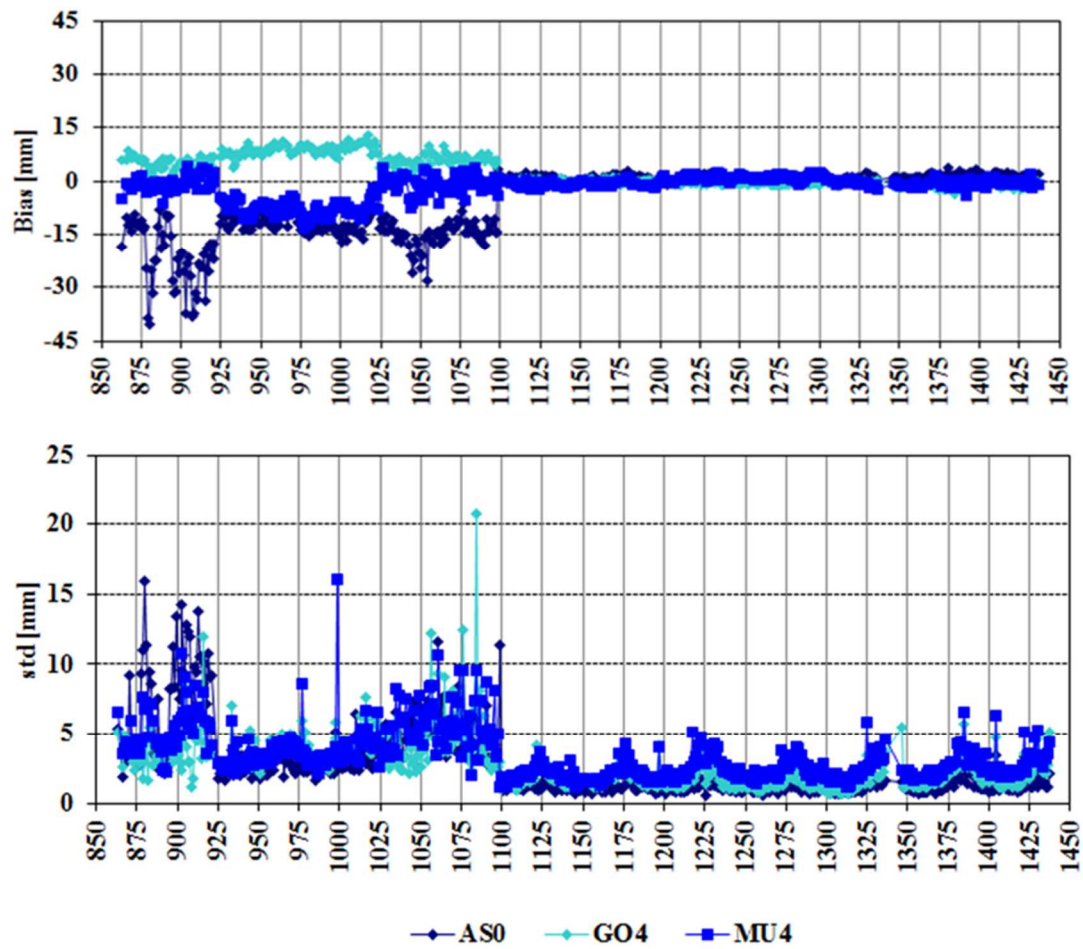
755



756

757 Figure 4. Left part: Time series of the ZTD and up component differences between two time series
 758 obtained with and without Non-Tidal Atmospheric Loading for two EPN stations: KIR0 (Kiruna,
 759 Sweden) and RIGA (Riga, Latvia). Right part: Correlation between these two parameters.

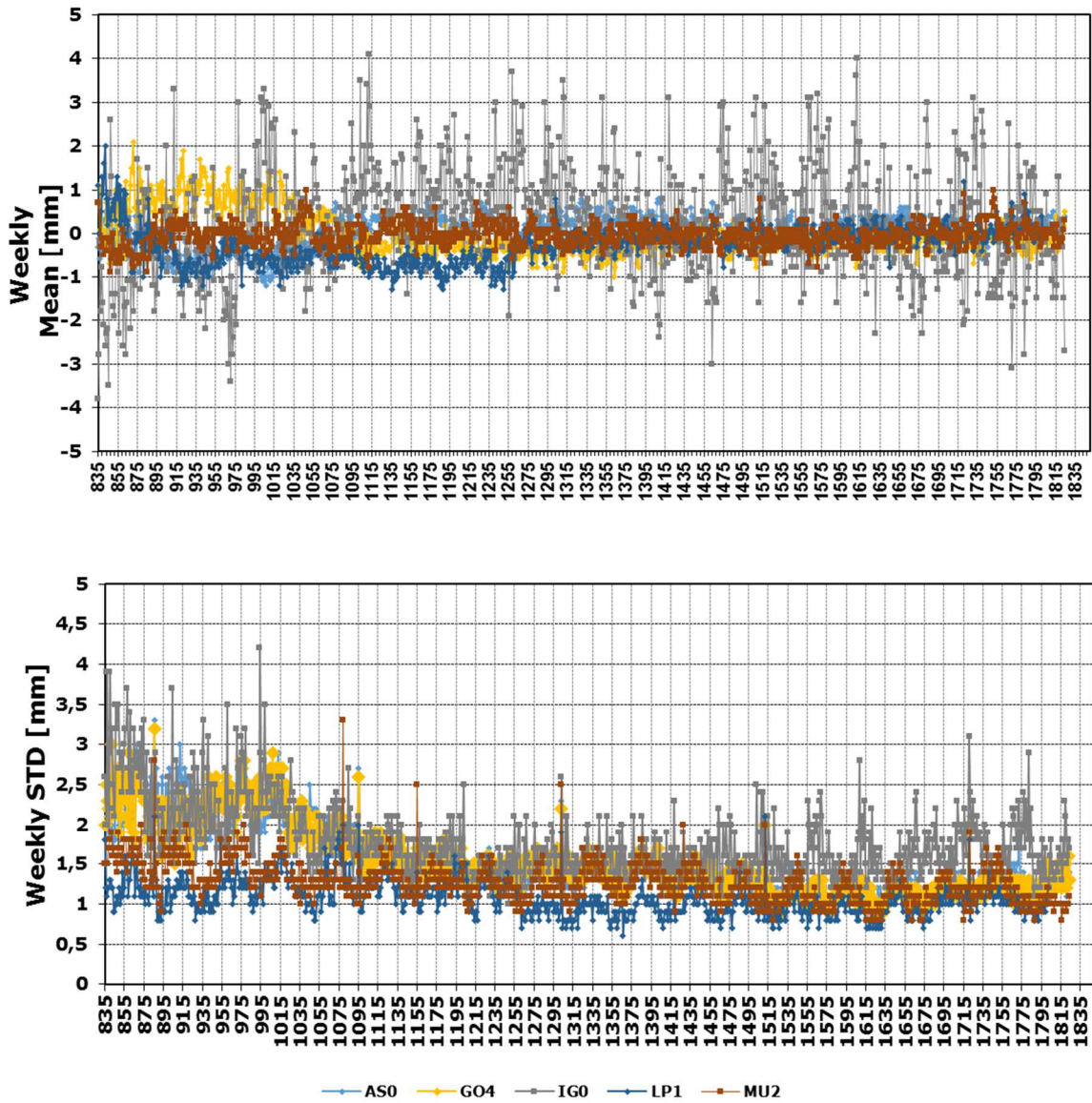
760



761

762 Figure 5 VENE (Venice Italy) time series of bias and standard deviation for the three contributing
 763 solutions AS0, GO4 and MU4 for the period July 21st, 1996 - July 28, 2007 (GPS week 0863-1437).
 764 GO0 and GO1 are not shown since they are very close to GO4.

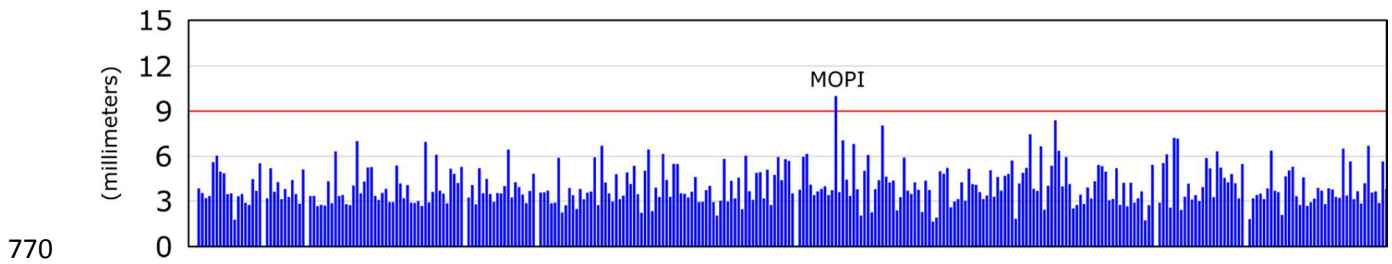
765

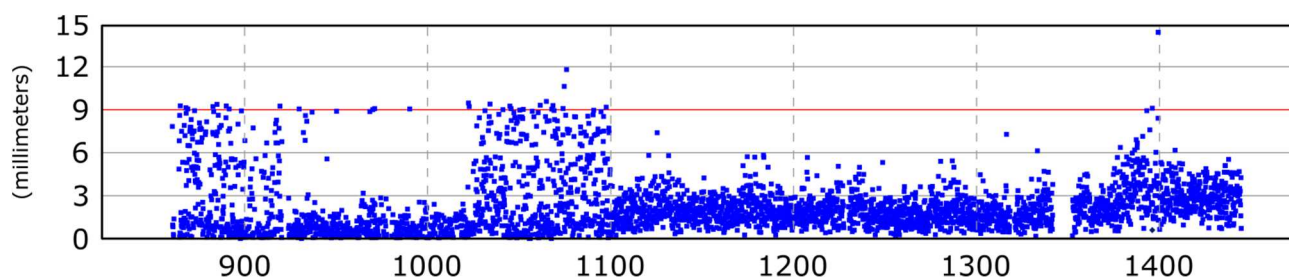


766

767 Figure 6 Weekly mean bias (upper part) and standard deviation (lower part) of each contribution
 768 solutions w.r.t. the final EPN Repro2 combination.

769

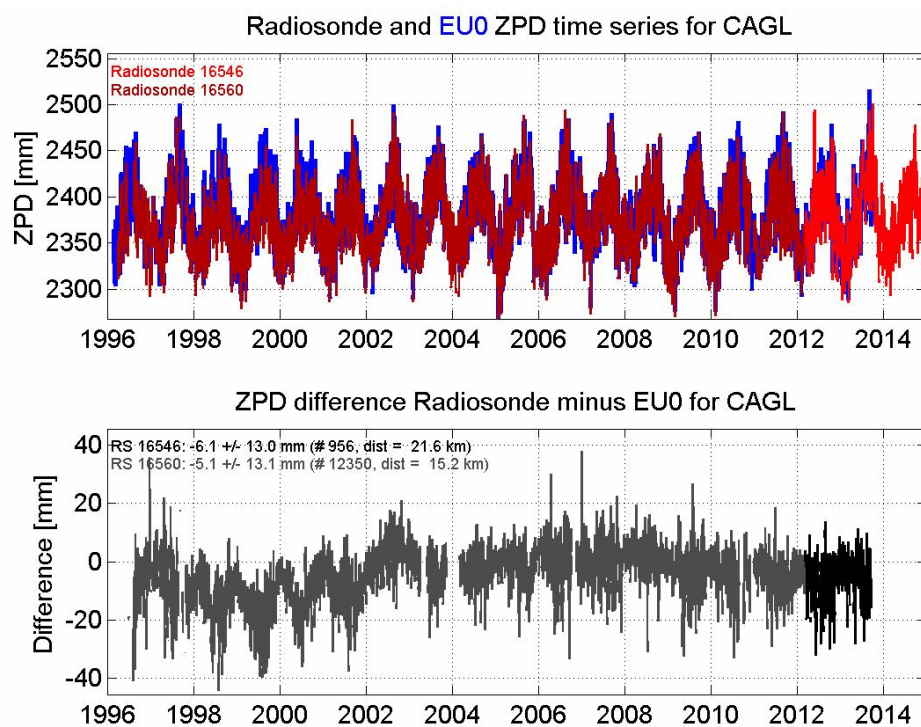




773

774 Figure 8 VENE (Venice Italy) time series of total consistency in up component for the period July
 775 21st, 1996 - July 28, 2007 (GPS week 0863-1437).

776

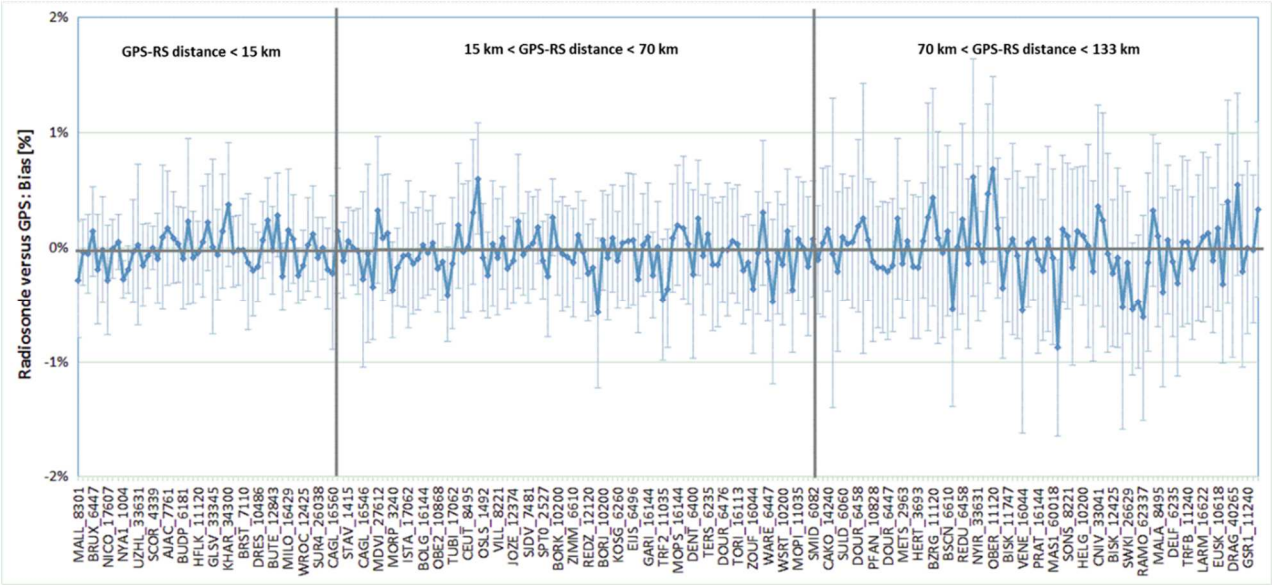


777

778 Figure 9 EPN station CAGL (Cagliari, Sardinia Island, Italy). Upper part: Radiosondes (in red) and
 779 GPS (in blue) ZTD time series. Lower part differences.

780

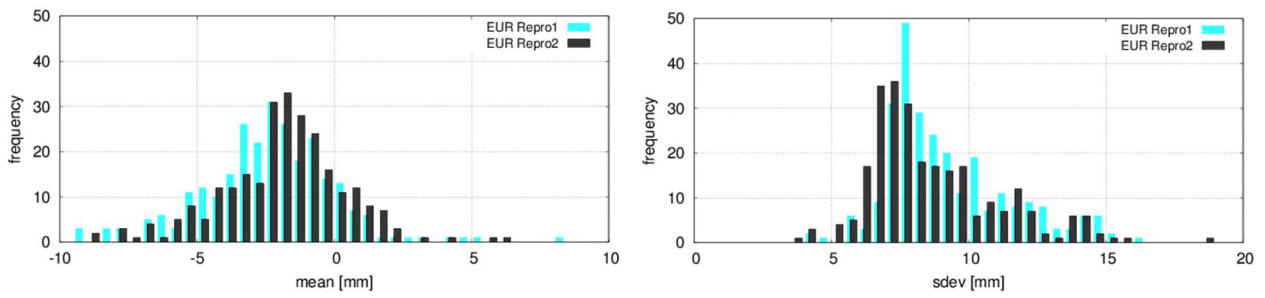
781



782

783 Figure 10 GPS versus Radiosonde Bias. The error bar is the standard deviation. Sites are sorted
784 according to the increasing distances from the nearest Radiosonde launch site. The x-axis
785 reports the GPS station and the Radiosonde code.

786

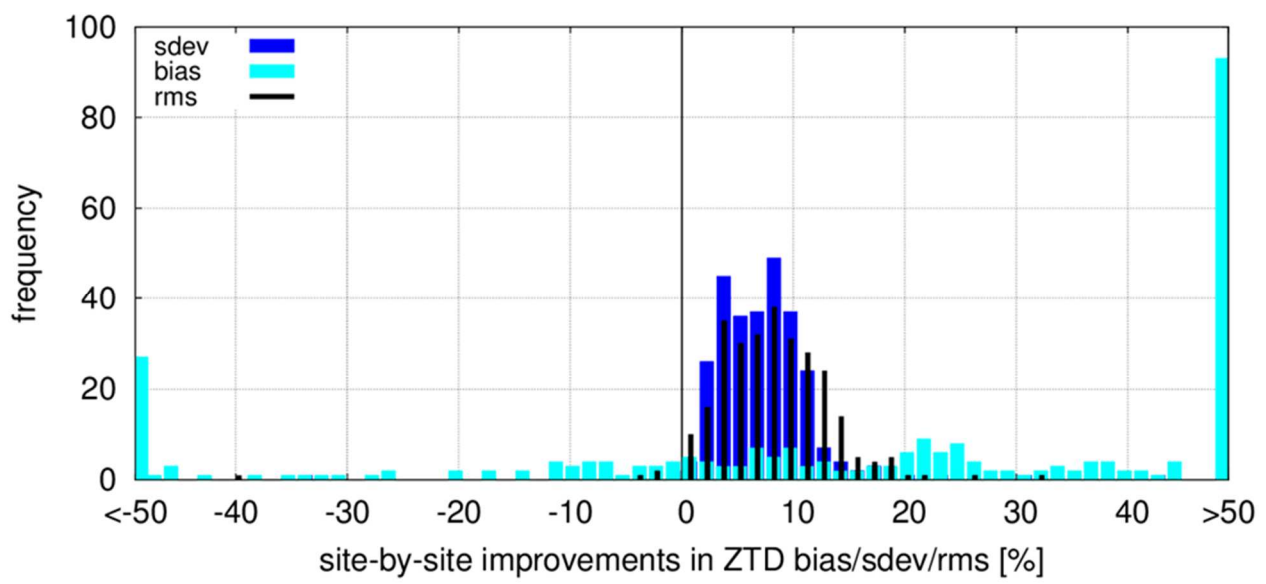


787

788 Figure 11: Distributions of station means (left) and standard deviations (right) of EPN Repro1 and
 789 Repro2 ZTDs compared to ERA-Interim ZTDs.

790

791

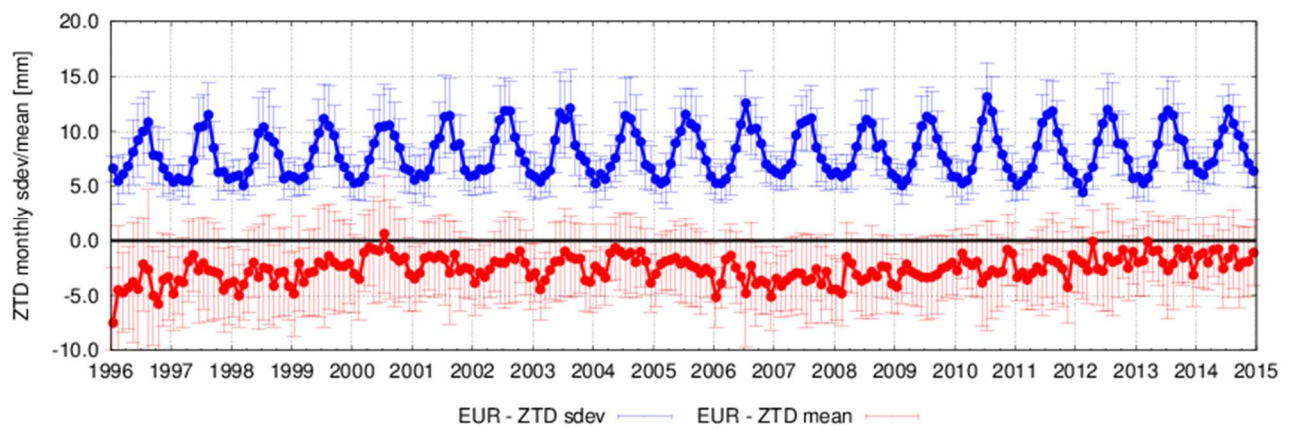


792

793 Figure 12: Site-by-site ZTD improvements of EPN Repro2 versus EPN Repro1 compared to ERA-
794 Interim

795

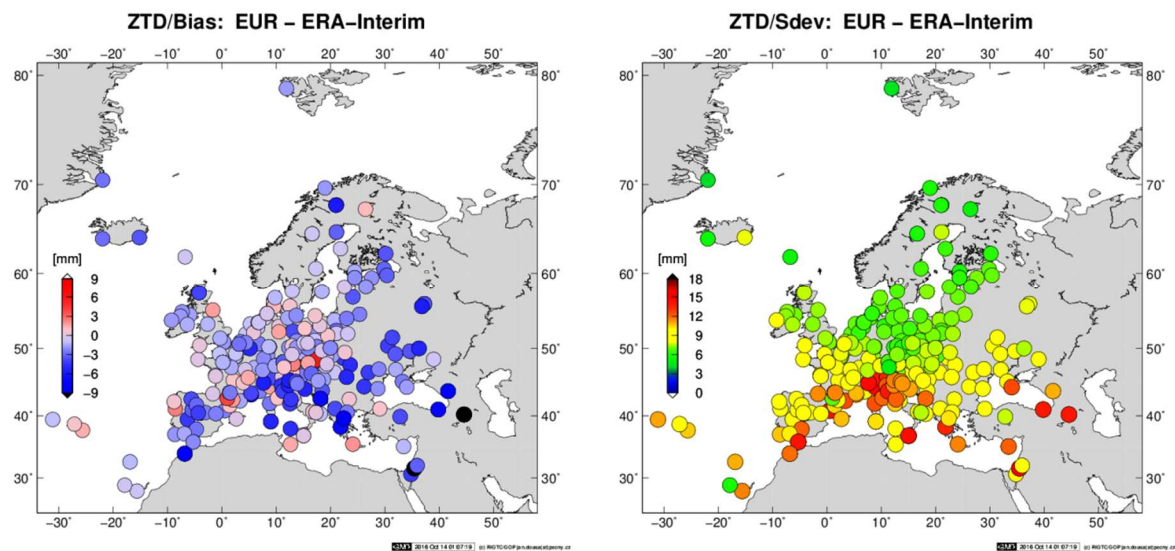
796



797

798 Figure 13: Time series of monthly mean biases (lower part) and standard deviations (upper part) for
799 ZTD differences of EPN Repro2 and NWM re-analysis. Uncertainties are calculated over all stations.

800

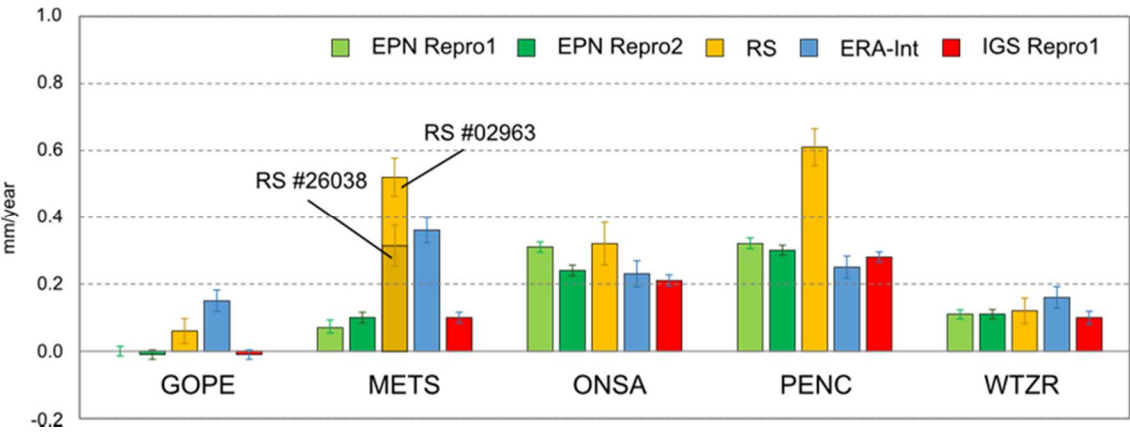


801

802 Figure 14: Geographical display of ZTD biases (left) and standard deviations (right) for EPN Repro2
 803 products compared to the ERA-Interim.

804

805



806

807 Figure 15: ZTD trend comparisons at five EPN stations. The error bars are the formal error of the
808 trend values.